# Isovector spin-multipole strength distributions in double-$\beta$-decay triplets

Lotta Jokiniemi* and Jouni Suhonen†
*Department of Physics, University of Jyvaskyla, P.O. Box 35 (YFL), FI-40014 Jyvaskyla, Finland*
(Received 5 April 2017; revised manuscript received 23 June 2017; published 8 September 2017)

In this work the energetics and strength distributions of isovector spin-dipole and spin-quadrupole transitions from the ground states of the pairs ($^{76}$Ge, $^{76}$Se), ($^{82}$Se, $^{82}$Kr), ($^{96}$Zr, $^{96}$Mo), ($^{100}$Mo, $^{100}$Ru), ($^{116}$Cd, $^{116}$Sn), ($^{128}$Te, $^{128}$Xe), ($^{130}$Te, $^{130}$Xe), and ($^{136}$Xe, $^{136}$Ba), of double-$\beta$-decay initial and final nuclei, to the $J^\pi = 0^-,1^-,2^-,1^+,2^+$, and $3^+$ excited states of the intermediate odd-odd nuclei $^{76}$As, $^{82}$Br, $^{96}$Nb, $^{100}$Tc, $^{116}$In, $^{128,130}$I, and $^{136}$Cs are investigated. The calculations are performed using a proton-neutron quasiparticle random-phase approximation (pnQRPA) theory framework with the Bonn-A two-body interaction in no-core single-particle valence spaces.

DOI: 10.1103/PhysRevC.96.034308

## I. INTRODUCTION

At present, the properties of neutrinos attract a lot of interest in the particle-physics and nuclear-physics communities. These properties can be studied in many ways, among others by the neutrino-oscillation experiments, the neutrino-nucleus scattering, and the neutrinoless double-$\beta$ ($0\nu\beta\beta$) decay [1–5]. The latter two processes require knowledge about nuclear properties in the form of the nuclear matrix elements (NMEs). The NMEs of these processes are built from real or virtual transitions between the ground state of an initial nucleus and the ground and excited states of a daughter nucleus. In particular, the transitions in the charged-current neutrino-nucleus scattering [6–8] and $0\nu\beta\beta$ share many common features, like the possibility to feed (highly) excited $J^\pi = 0^+,0^-,1^+,1^-,2^+,2^-,3^+,\ldots$ states of an odd-odd nucleus starting from the $0^+$ ground state of the neighboring even-even isobar. A suitable framework for studying these real or virtual transitions is the proton-neutron random-phase approximation (pnRPA) at closed nuclear major shells [9] and the corresponding theory for quasiparticles (pnQRPA) in the case of superfluid open-shell systems [10,11].

In the case of two-neutrino double-$\beta$ ($2\nu\beta\beta$) decay the NME consists of virtual Gamow-Teller (GT) transitions from the $0^+$ ground states of the initial and final even-even nuclei to the $1^+$ states of the intermediate nucleus. These transitions have typically been probed by the partial-wave $L = 0$ charge-exchange reactions (CXRs) by using the $\beta^-$ type of (p,n) or ($^3$He,t) reactions and $\beta^+$ type of (n,p), (d,$^2$He), or (t,$^3$He) reactions [12–14]. Results of these reaction studies can be compared with theoretical calculations of the Gamow-Teller and isovector spin-monopole (IVSM) strength distributions [15–17]. Lately, the partial-wave $L = 1$ CXRs to $2^-$ states have gained momentum by the improved experimental methods and facilities, e.g., the RCNP in Osaka, Japan [18]. These studies could be relevant for the $0\nu\beta\beta$ decays because a considerable portion of the corresponding NME can be built from virtual transitions via the $J^\pi = 2^-$ multipole states [19,20]. The experimental considerations can also be extended to the other $L = 1$ CXRs by studying the $\beta^-$ and $\beta^+$ types of feedings of the $0^-$ and $1^-$ states involved in the NMEs of the $0\nu\beta\beta$ decays.

In the present work we extend the study of [9] to open-shell superfluid nuclei relevant for the $0\nu\beta\beta$ decays. In [9] the pnRPA model was used for closed-shell nuclei to study the isovector spin-dipole (IVSD, $L = 1$) and spin-quadrupole (IVSQ, $L = 2$) $\beta^-$ and $\beta^+$ types of feeding of the $J^\pi = 0^-,1^-,2^-$ ($L = 1$) and $J^\pi = 1^+,2^+,3^+$ ($L = 2$) nuclear states in a few cases of odd-odd nuclei. Instead of the pnRPA, we adopt the pnQRPA (proton-neutron quasiparticle random-phase approximation) with partial restoration of the isospin symmetry [21] for our studies of the isovector spin-multipole $L = 1,2$ feeding of the nuclei $^{76}$As, $^{82}$Br, $^{96}$Nb, $^{100}$Tc, $^{116}$In, $^{128,130}$I, and $^{136}$Cs from the $0^+$ ground states of $^{76}$Ge, $^{82}$Se, $^{96}$Zr, $^{100}$Mo, $^{116}$Cd, $^{128,130}$Te, and $^{136}$Xe ($\beta^-$ type of feeding) and from the $0^+$ ground states of $^{76}$Se, $^{82}$Kr, $^{96}$Mo, $^{100}$Ru, $^{116}$Sn, $^{128,130}$Xe, and $^{136}$Ba ($\beta^+$ type of feeding). The feasibility of probing experimentally the IVSD $L = 1$ strength distributions to $J^\pi = 1^-,2^-$ states was demonstrated and experimental results are to be expected in the near future [18]. The feasibility of probing the IVSQ $L = 2$ strengths to $J^\pi = 1^+,2^+,3^+$ states is still an open question but could probably be done in the not so distant future. When and if available, the measured $L = 1$ and $L = 2$ strength distributions can be compared to the presently computed ones to learn more about the ability of the pnQRPA to describe the feeding of the important intermediate $J^\pi = 0^+,0^-,1^+,1^-,2^+,2^-,3^+$ multipole states in $0\nu\beta\beta$ processes.

The outline of this article is as follows: In Sec. II we introduce the used formalism, including the pnQRPA framework and transition amplitudes, in Sec. III we present and discuss the obtained results, and finally in Sec. IV we draw the final conclusions of the study.

## II. SHORT REVIEW OF THE FORMALISM

The formalism developed in [16], for the GT and isovector spin-monopole (IVSM) excitation modes, is now extended to the IVSD and IVSQ modes. At the same time we extend the corresponding studies of [9] to open-shell superfluid nuclei. The calculations start from the ground states of a number of selected even-even nuclei. In the present study we investigate the double-beta emitters in the triplets of isobars with $A = 76$, $A = 82$, $A = 96$, $A = 100$, $A = 116$, $A = 128$, $A = 130$,

*lotta.m.jokiniemi@student.jyu.fi
†jouni.suhonen@phys.jyu.fi

 

and $A = 136$. In the following subsections the stages of this step-by-step study are explained briefly.

### A. Single-particle bases

The single-particle energies for both protons and neutrons, for each even-even nucleus involved, are obtained by solving the radial Schrödinger equation for a Coulomb-corrected Woods-Saxon potential. The Woods-Saxon parameters are obtained from [22]. We include in our calculations only the bound and quasibound single-particle states.

In this work, the calculations are performed in large no-core single-particle bases, which means that all the states starting from $nl_j = 0s_{1/2}$ up to two oscillator major shells above the proton Fermi surface of each nucleus are taken into account. The same single-particle space is adopted also for neutrons.

### B. Quasiparticle spectra

The two-body interaction used in the BCS calculations is derived from the Bonn-A one-boson-exchange potential introduced in [23]. The BCS pairing gaps are fitted to the observed ones [24–26] using the three-point formulas,

$$\begin{aligned}\Delta_{\rm n}(A,Z) =& \tfrac{1}{4}(-1)^{A-Z+1}[S_{\rm n}(A+1,Z) - 2S_{\rm n}(A,Z) \\ &+ S_{\rm n}(A-1,Z)], \\ \Delta_{\rm p}(A,Z) =& \tfrac{1}{4}(-1)^{Z+1}[S_{\rm p}(A+1,Z+1) - 2S_{\rm p}(A,Z) \\ &+ S_{\rm p}(A-1,Z-1)],\end{aligned} \tag{1}$$

where $S_{\rm p}$ and $S_{\rm n}$ are the separation energies for protons and neutrons, respectively. This is achieved by adjusting the pairing strength parameters $g_{\rm pair}^{\rm (n)}$ and $g_{\rm pair}^{\rm (p)}$ which multiply the monopole $G$-matrix elements. The resulting pairing strength constants and pairing gaps are discussed in the next section.

### C. Spectra of the $J^\pi$ excitations in odd-odd nuclei

The wave functions and excitation energies for the complete set of $J^\pi$ excitations in the odd-odd nuclei are obtained by performing a pnQRPA diagonalization in the basis of unperturbed quasiproton-quasineutron pairs coupled to $J^\pi$. The pnQRPA states in odd-odd nuclei are then of the form,

$$\begin{aligned}|\omega\rangle &= Q_\omega^\dagger|{\rm pnQRPA}\rangle \\ &= \sum_{pn}\left[X_{pn}^\omega A_{pn}^\dagger(JM) - Y_{pn}^\omega \tilde{A}_{pn}(JM)\right]|{\rm pnQRPA}\rangle,\end{aligned} \tag{2}$$

where $\omega = nJ^\pi M$, $X$ and $Y$ are the forward- and backward-going amplitudes, $A^\dagger$ and $\tilde{A}$ the quasiproton-quasineutron creation and annihilation operators, and $|{\rm pnQRPA}\rangle$ is the pnQRPA vacuum. $M$ denotes the $z$ projection of $J$. The formalism is explained in detail in, e.g., [24,26].

The $X$ and $Y$ amplitudes of (2) are calculated by diagonalizing the pnQRPA matrix separately for each multipole $J^\pi$. The isoscalar ($T = 0$) and isovector ($T = 1$) parts of the particle-particle $G$-matrix elements are multiplied by common factors $g_{\rm pp}^{T=0}$ and $g_{\rm pp}^{T=1}$, respectively, for all the multipoles according to a method proposed in [21]. In addition, the particle-hole part was scaled by a common factor $g_{\rm ph}$ for all the multipoles. These renormalization factors are listed in the following section for each mass number separately.

### D. Transition operators and strength distributions

The transition operators for the spin-dipole ($L = 1$) and spin-quadrupole ($L = 2$) transitions are of the form,

$$Q_{L,J}^\pm = r^L[\boldsymbol{Y}_L\boldsymbol{\sigma}]_J i^L t_\pm, \tag{3}$$

where $Y_L$ is the spherical harmonic of rank $L$, $\boldsymbol{\sigma}$ the Pauli spin tensor operator, and $t_+$ and $t_-$ are the isospin raising and lowering operators. The reduced single-particle NMEs of this operator are of the form [22,24],

$$\begin{aligned}(j_f||\mathcal{O}_{L,J}^\pm||j_i) &= \left(n_f l_f \tfrac{1}{2} j_f||r^L[\boldsymbol{Y}_L\boldsymbol{\sigma}]_J i^L||n_i l_i \tfrac{1}{2} j_i\right) \\ &= \sqrt{6}\hat{j}_f\hat{J}\hat{j}_i\frac{(-1)^{l_f}}{\sqrt{4\pi}}\hat{l_f}\hat{L}\hat{l_i}\begin{pmatrix} l_f & L & l_i \\ 0 & 0 & 0\end{pmatrix} \\ &\times\begin{Bmatrix} l_f & \frac{1}{2} & j_f \\ l_i & \frac{1}{2} & j_i \\ L & 1 & J\end{Bmatrix}\mathcal{R}_{fi}^{(L)}(-1)^{\frac{1}{2}(l_i-l_f+L)},\end{aligned} \tag{4}$$

where $\mathcal{R}_{fi}^{(L)}$ is a radial integral [24] and the effect of the isospin ladder operators is taken into account by the fact that the initial $j_i = (n_i l_i \frac{1}{2} j_i)$ and final $j_f = (n_f l_f \frac{1}{2} j_f)$ single-particle states have different isospin projections. Here $n$ denotes the principal quantum number, $l$ the orbital angular momentum, and $j$ the total angular momentum. Now the reduced NMEs can be calculated from [24]

$$(J^\pi||\mathcal{O}_{L,J}^\pm||0^+) = \sum_{ab}\frac{(a||\mathcal{O}_{L,J}^\pm||b)}{\sqrt{2J+1}}(J^\pi||[c_a^\dagger\tilde{c}_b]_J||0^+), \tag{5}$$

where $b$ and $a$ denote the initial and final single-particle quantum numbers.

The transition strength for a transition from a $0^+$ ground state to the $i$th $J^\pi$ state can be calculated from

$$S_{LJ}^\pm(i) = |(J_i^\pi||\mathcal{O}_{L,J}^\pm||0^+)|^2. \tag{6}$$

## III. RESULTS AND DISCUSSION

In this chapter we present and discuss the results and the methods used in the calculations.

### A. Single-particle bases and energies

We created the single-particle bases by solving the eigenstates of the Woods-Saxon potential for protons and neutrons, separately (for protons we corrected the potential with the Coulomb force). The values for the central, orbital, and spin-orbit parameters, and the radius and the surface thickness parameters needed in the calculations were taken from [22]. Small adjustments to the proton and neutron single-particle energies were done for the orbitals close to the Fermi surfaces to better reproduce the low-lying spectra of the neighboring odd-mass nuclei. Because we are dealing with no-core calculations, we take all the orbits from the $N = 0$ oscillator major shell up to about two oscillator major shells above the respective Fermi surfaces for protons and neutrons.

TABLE I. Pairing scaling factors and the resulting pairing gaps for the nuclei relevant for this work.

| Nucleus | $g_{\rm pair}^{(\rm n)}$ | $g_{\rm pair}^{(\rm p)}$ | $\Delta_{\rm n}$(MeV) | $\Delta_{\rm p}$(MeV) |
|---|---|---|---|---|
| $^{76}$Ge | 0.97 | 0.89 | 1.57 | 1.52 |
| $^{76}$Se | 1.01 | 0.91 | 1.72 | 1.71 |
| $^{82}$Se | 0.94 | 0.84 | 1.51 | 1.43 |
| $^{82}$Kr | 1.01 | 0.86 | 1.65 | 1.63 |
| $^{96}$Zr | 0.77 | 0.85 | 0.92 | 1.48 |
| $^{96}$Mo | 0.90 | 0.93 | 1.03 | 1.52 |
| $^{100}$Mo | 0.88 | 0.96 | 1.31 | 1.63 |
| $^{100}$Ru | 0.85 | 0.93 | 1.27 | 1.60 |
| $^{116}$Cd | 0.89 | 0.93 | 1.37 | 1.43 |
| $^{116}$Sn | 0.82 | 0.89 | 1.16 | 1.84 |
| $^{128}$Te | 0.86 | 0.81 | 1.30 | 1.09 |
| $^{128}$Xe | 0.86 | 0.88 | 1.27 | 1.30 |
| $^{130}$Te | 0.86 | 0.78 | 1.21 | 1.02 |
| $^{130}$Xe | 0.85 | 0.86 | 1.25 | 1.26 |
| $^{136}$Xe | 0.84 | 0.76 | 1.44 | 0.98 |
| $^{136}$Ba | 0.87 | 0.83 | 1.08 | 1.22 |

An example of the single-particle orbitals and energies for the $A = 76$ system is shown in Table I in [17].

### B. Pairing gaps, quasiparticle spectra, and BCS occupation factors

The two-body matrix elements obtained from the Bonn-A interaction were applied to the "left-hand-side" and "right-hand-side" even-even nuclei by renormalizing the monopole neutron and proton channels, separately. The scaling factors $g_{\rm pair}^{(\rm n)}$ and $g_{\rm pair}^{(\rm p)}$ were adjusted to reproduce the phenomenological pairing gaps given in Eq. (1). The needed neutron (proton) separation energies $S_{\rm n}$ ($S_{\rm p}$) were taken from [27] and [28]. The scaling factors and the resulting pairing gaps for the nuclei of interest are listed in Table I. Using these scaling factors we performed the BCS calculations and obtained the one-quasiparticle spectra and occupation factors $v$ and vacancy factors $u$ needed in the subsequent pnQRPA calculations of the energies and wave functions. These factors, along with the pnQRPA amplitudes of (2), are used to construct the one-body transition densities of (5) in the form [24],

$$(J^\pi||[c_p^\dagger \tilde{c}_n]_J||0^+) = \widehat{J}\left(u_p v_n X_{pn}^\omega + v_p u_n Y_{pn}^\omega\right), \quad (7)$$

$$(J^\pi||[c_n^\dagger \tilde{c}_p]_J||0^+) = \widehat{J}(-1)^J\left(v_p u_n X_{pn}^\omega + u_p v_n Y_{pn}^\omega\right). \quad (8)$$

### C. Energy spectra and IVSD and IVSQ strength distributions

We decompose each isobaric triplet with mass number $A$ to "left-hand-side" even-even $(A,N,Z)$, "right-hand-side" even-even $(A,N-2,Z+2)$, and "intermediate" odd-odd $(A,N-1,Z+1)$ nuclei. We construct the spectra of $J^\pi$ excitations in the intermediate odd-odd nuclei applying the pnQRPA formalism [25,26,29], including particle-hole and particle-particle channels, to the left- and right-hand-side even-even nuclei. In this way we obtain two sets of energies and wave functions for each $J^\pi$ state.

TABLE II. Renormalization factors for the particle-hole and particle-particle interactions in different nuclei.

| $A$ | $g_{\rm ph}$ | $g_{\rm pp}^{T=0}$ | $g_{\rm pp}^{T=1}$ |
|---|---|---|---|
| 76 | 1.156 | 0.83 | 0.96 |
| 82 | 0.997 | 0.82 | 0.95 |
| 96 | 1.415 | 0.89 | 0.94 |
| 100 | 1.224 | 0.875 | 0.91 |
| 116 | 1.518 | 0.82 | 0.81 |
| 128 | 1.267 | 0.745 | 0.87 |
| 130 | 1.228 | 0.73 | 0.86 |
| 136 | 1.262 | 0.67 | 0.87 |

The values of the particle-hole (particle-particle) renormalization factors $g_{\rm ph}$ ($g_{\rm pp}^{T=0,1}$) are listed in Table II. The $g_{\rm ph}$ values were fitted to reproduce the energetics of the "left-hand-side" GT$^-$ giant resonance (GTGR). The $g_{\rm pp}$ values have usually been fixed by the half-lives of $2\nu\beta\beta$ decays [30–34], by the $\log ft$ values of $\beta$ decays [35,36], or by both $\beta$ and $2\nu\beta\beta$ decays [37,38]. In this work, we adopt an improved method, quasiparticle random phase approximation with partial restoration of the isospin symmetry, introduced in [19], and first proposed in [21]: We decompose the pnQRPA NMEs into isoscalar ($T = 0$) and isovector ($T = 1$) parts and then adjust the parameters $g_{\rm pp}^{T=0}$ and $g_{\rm pp}^{T=1}$ independently. The isovector parameter $g_{\rm pp}^{T=1}$ is adjusted so that the Fermi NME of $2\nu\beta\beta$ matrix element vanishes, and thus the isospin symmetry is restored. Then we independently vary the isoscalar parameter $g_{\rm pp}^{T=0}$ such that it reproduces the calculated matrix element corresponding to the measured $2\nu\beta\beta$ half-life and a slightly quenched value $g_{\rm A} = 1.0$ of the axial vector coupling constant. These values are determined for each mass number separately, and the obtained parameters are adopted for all the multipoles in both left- and right-hand-side even-even nuclei. The bare value $g_{\rm A} = 1.27$ was also tested in the determination of the $g_{\rm pp}^{T=0}$ parameters, but the parameter values obtained this way differed only by 0.01–0.03 from those obtained with $g_{\rm A} = 1.0$, resulting in less than 0.3-MeV differences in the obtained energy centroids of the spin-multipole giant resonances. Because the changes in the energy centroids were so minor, we do not list separately the results for $g_{\rm A} = 1.27$.

### D. Energy centroids and strength functions for the spin-dipole and spin-quadrupole excitations

In this section we discuss the strength distributions of the IVSD and IVSQ excitations for the left-hand-side (IVSD$^-$ and IVSQ$^-$) and right-hand-side (IVSD$^+$ and IVSQ$^+$) initial ground states. The corresponding strength functions are

$$S(\text{IVSD}^-)(i) = |(J_i^\pi||\mathcal{O}_{1,J}^-||0_{\rm L}^+)|^2, \quad (9)$$

$$S(\text{IVSD}^+)(i) = |(J_i^\pi||\mathcal{O}_{1,J}^+||0_{\rm R}^+)|^2, \quad (10)$$

$$S(\text{IVSQ}^-)(i) = |(J_i^\pi||\mathcal{O}_{2,J}^-||0_{\rm L}^+)|^2, \quad (11)$$

$$S(\text{IVSQ}^+)(i) = |(J_i^\pi||\mathcal{O}_{2,J}^+||0_{\rm R}^+)|^2, \quad (12)$$

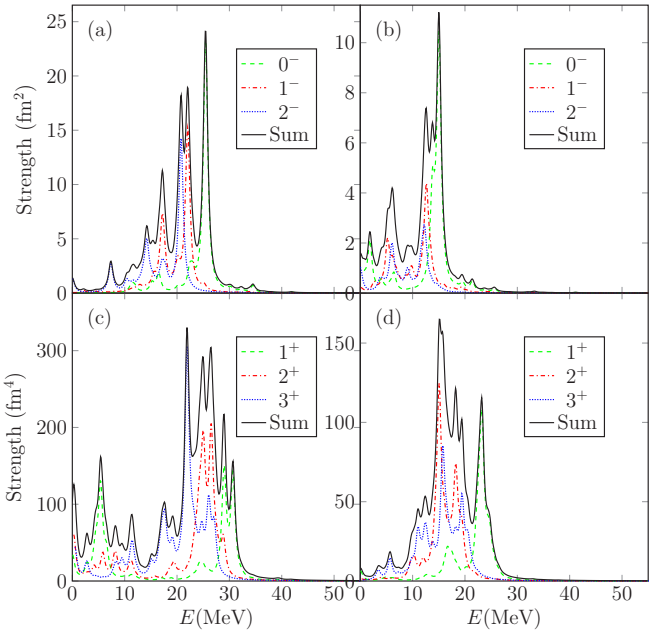


FIG. 1. Strength distributions for $A = 76$. (a) $L = 1, \beta^-$, (b) $L = 1, \beta^+$, (c) $L = 2, \beta^-$, (d) $L = 2, \beta^+$. The solid line denotes the sum of the dashed, dotted, and dash-dotted individual contributions. Energies are measured relative to the ground state of the odd-odd final nucleus. The strengths are given in units of fm$^2$ for $J^\pi = 0^-, 1^-, 2^-$ and in fm$^4$ for $J^\pi = 1^+, 2^+, 3^+$.

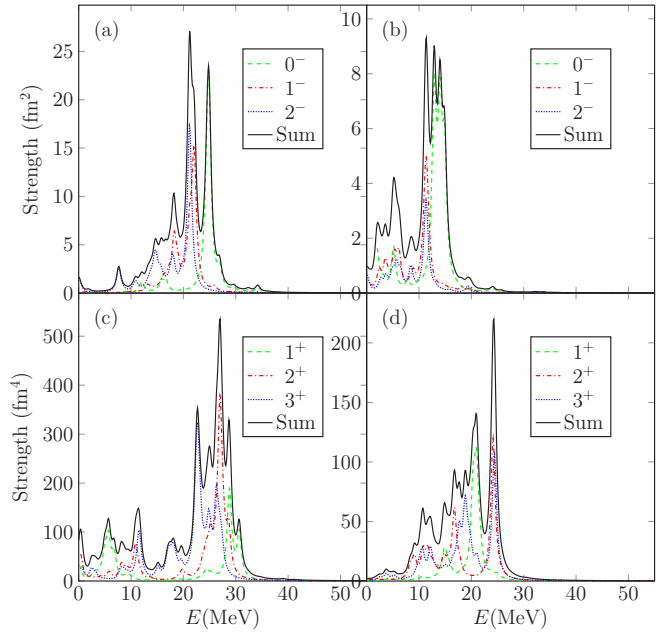


FIG. 2. The same as in Fig. 1 for $A = 82$.

where the transition operator is given in (3), $0^+_{\rm L}$ ($0^+_{\rm R}$) is the ground state of the left-hand-side (right-hand-side) even-even nucleus, and $J^\pi_i$ is the $i$th $J^\pi$ state in the intermediate odd-odd nucleus.

The resulting strength distribution is discrete because of the discrete basis used in the calculation. To make it better comparable with the experimental distribution we fold it with the Lorentzian folding function [39],

$$F_L(E - E_0) = \frac{W}{\pi} \frac{1}{W^2 + (E - E_0)^2}, \tag{13}$$

where $E$ is the excitation energy in the odd-odd final nucleus, $E_0$ the energy of the pnQRPA phonon corresponding to a peak, and $W$ the width of this Lorentz peak. For the width we have chosen the value $W = 0.5$ MeV. The folded strength distributions are shown in Figs. 1–8 for different mass numbers. In the (a) panels the strength distributions of IVSD$^-$ transitions to different multipoles are shown, in the (b) panels the corresponding strength distributions of IVSD$^+$ transitions are shown, and in the (c) and (d) panels the IVSQ$^-$ and IVSQ$^+$ transitions to different multipoles are shown. The energies are given in MeV with respect to the ground state of the odd-odd final nucleus and the solid line gives the sum distribution by adding the dashed, dotted, and dash-dotted individual contributions. The strengths are given in units of fm$^2$ for the $L = 1$ ($J^\pi = 0^-, 1^-, 2^-$) transitions and in fm$^4$ for the $L = 2$ ($J^\pi = 1^+, 2^+, 3^+$) transitions.

We note that for $L = 1$ $\beta^-$ transitions the average energy is highest for $0^-$ excitations, except for a few exceptions, lowest for $2^-$ excitations. This effect was also noted in the earlier calculations [9,40,41]. It can also be noted that the strength for $J^\pi = 0^-, 1^-$ is concentrated in a few peaks, whereas the strength for $J^\pi = 2^-$ is more spread. This was noted also in [9].

Similar effects can be seen in the case of $L = 2$ $\beta^-$ transitions: The $1^+$ excitations are the highest in energy, whereas the $3^+$ excitations are the lowest. As noted in [9], most of the strength of $J^\pi = 1^+$ resonances is carried by a few peaks, whereas for the $J^\pi = 2^+, 3^+$ excitations the strength distributions are much more fragmented. This effect becomes more visible for the heavier masses.

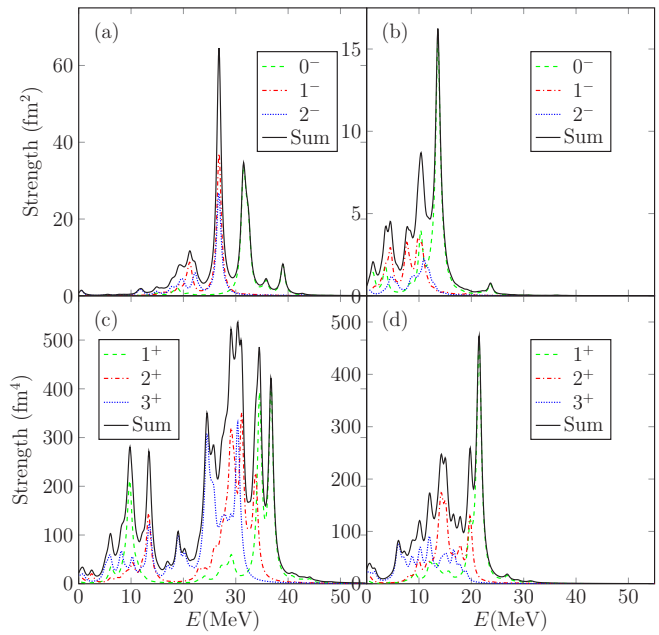


FIG. 3. The same as in Fig. 1 for $A = 96$.

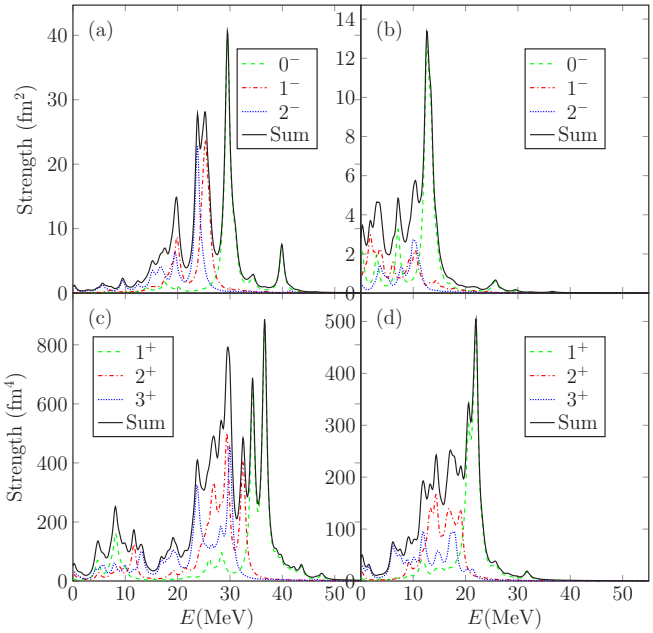


FIG. 4. The same as in Fig. 1 for $A = 100$.

In Table III we present the calculated energy centroids for IVSD$^{\pm}$ and IVSQ$^{\pm}$ transitions for different multipoles and mass numbers. The energies are again given with respect to the odd-odd final nucleus. For the $\beta^-$ type of strength the spin-multipole giant resonance (SMGR) region forms a more or less isolated island so that the total strength of the GR region can be separated from the low-energy one. This is why in Table III the spin-multipole strength of the SMGR is only part of the total $\beta^-$ strength $S^-_{\rm tot}$. For the $\beta^+$ type of transitions such a separation is not easy and hence only the total strength $S^+_{\rm tot}$ is given.

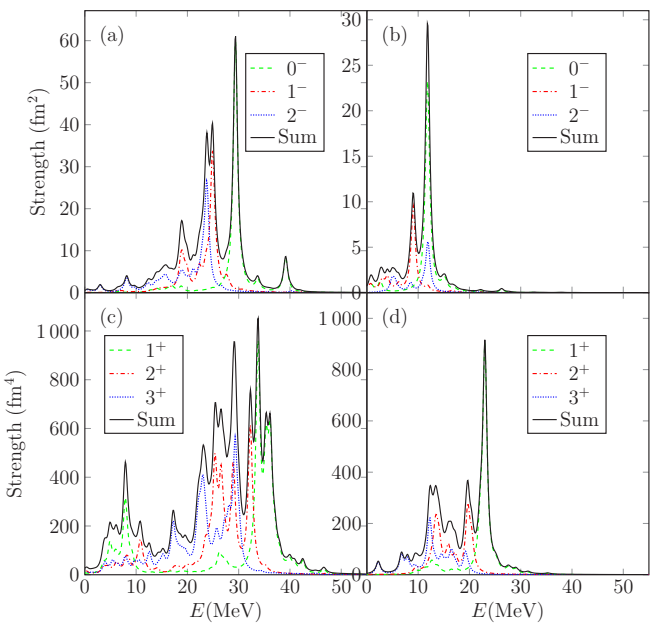


FIG. 5. The same as in Fig. 1 for $A = 116$.

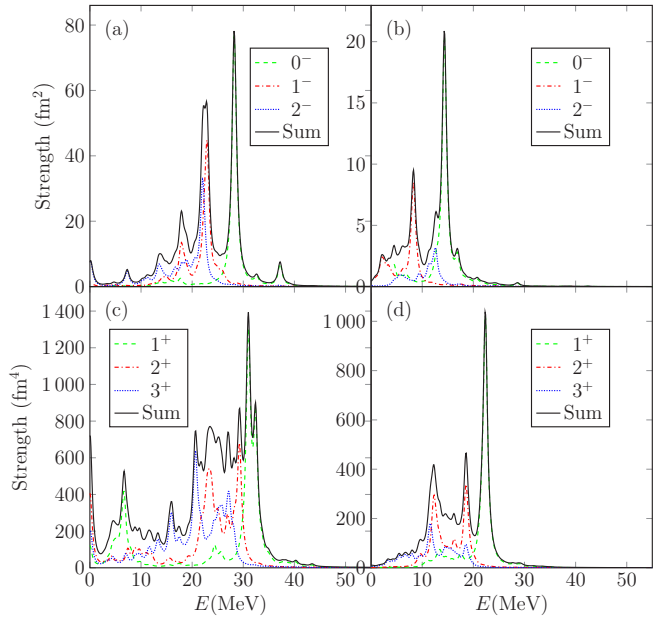


FIG. 6. The same as in Fig. 1 for $A = 128$.

From Table III we see that for $L = 1$ transitions the strengths $S^-_{\rm tot}$ and $S^+_{\rm tot}$ are largest for $0^-$ transitions and smallest for $2^-$ transitions, except for the $A = 82$ system. This kind of trend was also noted in [9] for closed-shell nuclei. In [9] it was seen that for $L = 2$ transitions the strengths $S^-_{\rm tot}$ and $S^+_{\rm tot}$ are largest for $1^+$ transitions and smallest for $3^+$ transitions. Our results for $S^-_{\rm tot}$ and $S^+_{\rm tot}$ differ from [9] for mass numbers $A = 76$ and 82, and $S^-_{\rm tot}$ for mass numbers $A = 96, 128, 130,$ and 136. Only for $A = 116$ and 100 our results agree with [9]. The deviations from the IVSD results of [9] are most likely related to the fact that in the present work we discuss open-shell nuclei, not magic nuclei as in [9].

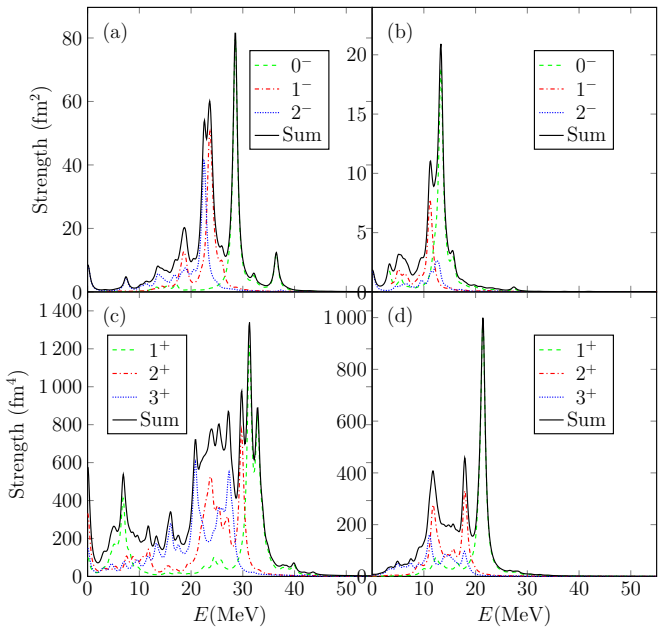


FIG. 7. The same as in Fig. 1 for $A = 130$.

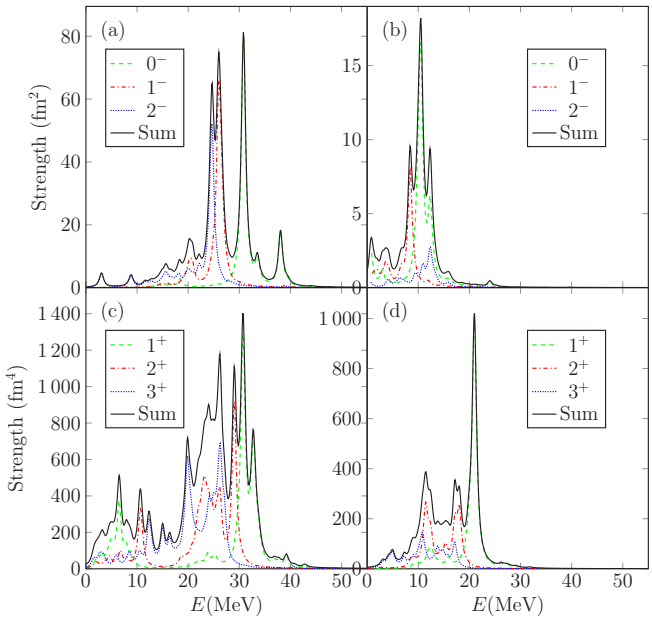


FIG. 8. The same as in Fig. 1 for $A = 136$.

## IV. CONCLUSIONS

In this work we have performed realistic pnQRPA calculations of the isovector spin-dipole and spin-quadrupole excitations in odd-odd nuclei belonging to double-$\beta$-decay triplets with $A = 76$, $A = 82$, $A = 96$, $A = 100$, $A = 116$, $A = 128$, $A = 130$, and $A = 136$. The calculations were performed in large no-core single-particle bases with realistic Bonn-A-type two-body interactions. The couplings of the pairing monopole channels were adjusted to reproduce the experimental odd-even mass differences separately for protons and neutrons. Furthermore, the proton-neutron particle-hole renormalization factor was fitted to the energy of the GTGR centroids of the left-hand-side even-even nuclei. The isovector and isoscalar particle-particle strengths were fitted to reproduce the observed $2\nu\beta\beta$ half-lives and to restore the isospin symmetry of the $2\nu\beta\beta$ transitions, as proposed in [21].

The resulting strength distributions of orbital angular momentum $L = 1,2$ transitions were computed and plotted for the multipole $J^\pi = 0^-,1^+,1^-,2^+,2^-,3^+$ states in the odd-odd intermediate nuclei. From these distributions we can see that there is a considerable difference in the giant-resonance energy centroids of the various $J$ states corresponding to a given $L$. For $L = 1$ transitions the transition strengths were highest for the lowest-$J$ transitions and lowest for the highest-$J$ transitions, except for $A = 82$. For $L = 2$ transitions there was no clear ordering for the transition strengths.

In the future, having access to experimental data on the $L = 1$ (and possibly $L = 2$) strength functions, one could make comparisons with the present and future theoretical calculations and access the validity of, e.g., the model Hamiltonians and their predicted isovector spin-multipole distributions and giant resonance properties.

TABLE III. Energy centroids of SMGRs and transition strengths $S^{\pm}$(GR) of the corresponding $\beta^-$ and $\beta^+$ transitions for different mass numbers. Also the total strengths $S^{\pm}_{\rm tot}$ are given. The strengths are given in units of fm$^2$ for $J^\pi = 0^-,1^-,2^-$ and in fm$^4$ for $J^\pi = 1^+,2^+,3^+$.

| $A$ | $J^\pi$ | $E(\mathrm{GR})_-$ (MeV) | $S^-$(GR) | $S^-_{\rm tot}$ | $E(\mathrm{GR})_+$ (MeV) | $S^+_{\rm tot} = S^+$(GR) |
|---|---|---|---|---|---|---|
| 76 | $0^-$ | 18.752 | 48.168 | 50.360 | 11.623 | 30.945 |
| | $1^-$ | 14.751 | 47.910 | 48.785 | 6.871 | 21.143 |
| | $2^-$ | 16.639 | 39.080 | 45.333 | 10.225 | 12.391 |
| | $1^+$ | 26.502 | 529.73 | 834.15 | 20.199 | 370.39 |
| | $2^+$ | 22.406 | 1017.3 | 1220.3 | 16.455 | 485.92 |
| | $3^+$ | 19.285 | 1295.8 | 1496.2 | 13.101 | 550.41 |
| 82 | $0^-$ | 17.339 | 47.873 | 50.305 | 10.388 | 32.835 |
| | $1^-$ | 14.300 | 52.503 | 53.505 | 7.197 | 22.323 |
| | $2^-$ | 15.798 | 47.021 | 52.472 | 10.218 | 12.758 |
| | $1^+$ | 25.493 | 512.94 | 847.96 | 19.542 | 383.65 |
| | $2^+$ | 23.201 | 1080.6 | 1441.6 | 19.395 | 511.23 |
| | $3^+$ | 19.387 | 1385.8 | 1815.7 | 18.018 | 604.18 |
| 96 | $0^-$ | 31.703 | 99.535 | 99.695 | 11.914 | 41.175 |
| | $1^-$ | 24.954 | 82.338 | 82.990 | 7.810 | 23.343 |
| | $2^-$ | 22.720 | 66.923 | 71.897 | 8.325 | 12.496 |
| | $1^+$ | 33.900 | 1485.8 | 1987.0 | 19.959 | 1128.7 |
| | $2^+$ | 27.214 | 2137.8 | 2306.3 | 14.967 | 963.80 |
| | $3^+$ | 24.002 | 2108.2 | 2440.8 | 10.803 | 816.56 |
| 100 | $0^-$ | 25.639 | 104.54 | 105.21 | 11.532 | 46.076 |
| | $1^-$ | 19.847 | 86.159 | 87.810 | 7.356 | 27.033 |
| | $2^-$ | 18.487 | 69.902 | 74.454 | 8.673 | 13.785 |
| | $1^+$ | 31.196 | 2946.2 | 3447.2 | 20.938 | 1629.2 |
| | $2^+$ | 24.227 | 2644.2 | 3088.6 | 15.122 | 1212.2 |
| | $3^+$ | 21.248 | 2405.9 | 2842.4 | 11.063 | 925.65 |
| 116 | $0^-$ | 29.069 | 123.49 | 124.29 | 11.537 | 42.862 |
| | $1^-$ | 22.780 | 107.91 | 108.56 | 7.215 | 24.937 |
| | $2^-$ | 21.002 | 89.649 | 100.83 | 9.278 | 15.684 |
| | $1^+$ | 34.214 | 3541.6 | 4450.9 | 22.103 | 1920.6 |
| | $2^+$ | 27.367 | 3559.4 | 4084.1 | 16.253 | 1411.7 |
| | $3^+$ | 24.327 | 3567.6 | 4021.4 | 12.840 | 1140.8 |
| 128 | $0^-$ | 22.888 | 156.98 | 160.33 | 10.189 | 47.981 |
| | $1^-$ | 16.943 | 135.86 | 138.30 | 6.841 | 26.435 |
| | $2^-$ | 17.069 | 108.12 | 121.01 | 9.774 | 14.658 |
| | $1^+$ | 28.038 | 3733.4 | 4771.9 | 21.330 | 2204.5 |
| | $2^+$ | 22.628 | 3749.4 | 4613.8 | 16.018 | 1595.0 |
| | $3^+$ | 19.087 | 4166.9 | 4861.7 | 12.939 | 1153.4 |
| 130 | $0^-$ | 25.108 | 165.89 | 169.18 | 11.614 | 46.475 |
| | $1^-$ | 19.342 | 143.27 | 147.54 | 8.517 | 25.007 |
| | $2^-$ | 17.058 | 116.69 | 130.18 | 9.369 | 13.620 |
| | $1^+$ | 27.796 | 3842.5 | 4973.5 | 20.950 | 2201.8 |
| | $2^+$ | 22.648 | 3918.9 | 4870.3 | 16.058 | 1574.0 |
| | $3^+$ | 19.252 | 4443.6 | 5207.7 | 12.798 | 1103.3 |
| 136 | $0^-$ | 29.610 | 180.57 | 180.63 | 9.858 | 44.987 |
| | $1^-$ | 23.886 | 158.95 | 159.29 | 6.812 | 23.770 |
| | $2^-$ | 21.631 | 132.88 | 149.85 | 9.146 | 13.265 |
| | $1^+$ | 28.709 | 3897.1 | 5163.8 | 20.268 | 2220.1 |
| | $2^+$ | 23.065 | 4627.8 | 5112.8 | 15.707 | 1584.7 |
| | $3^+$ | 20.234 | 5004.4 | 5498.7 | 12.231 | 1094.8 |

**ACKNOWLEDGMENTS**

This work was partially supported by the Academy of Finland under the Finnish Centre of Excellence Programme 2012-2017 (Nuclear and Accelerator Based Programme at JYFL).

[1] H. Ejiri, Phys. Rep. **338**, 265 (2000).
[2] F. T. Avignone, S. R. Elliot, and J. Engel, Rev. Mod. Phys. **80**, 481 (2008).
[3] J. D. Vergados, H. Ejiri, and F. Šimkovic, Rep. Prog. Phys. **75**, 106301 (2012).
[4] J. Suhonen and O. Civitarese, Phys. Rep. **300**, 123 (1998).
[5] J. Maalampi and J. Suhonen, Adv. High Energy Phys. **2013**, 505874 (2013).
[6] E. Ydrefors and J. Suhonen, Phys. Rev. C **87**, 034314 (2013).
[7] W. Almosly, B. G. Carlsson, J. Dobaczewski, J. Suhonen, J. Toivanen, P. Vesely, and E. Ydrefors, Phys. Rev. C **89**, 024308 (2014).
[8] W. Almosly, B. G. Carlsson, J. Suhonen, J. Toivanen, and E. Ydrefors, Phys. Rev. C **94**, 044614 (2016).
[9] N. Auerbach and A. Klein, Phys. Rev. C **30**, 1032 (1984).
[10] J. Suhonen and O. Civitarese, J. Phys. G **39**, 085105 (2012).
[11] J. Suhonen and O. Civitarese, J. Phys. G **39**, 124005 (2012).
[12] P. Puppe, D. Frekers, T. Adachi, H. Akimune, N. Aoi, B. Bilgier, H. Ejiri, H. Fujita, Y. Fujita, M. Fujiwara, E. Ganioğlu, M. N. Harakeh, K. Hatanaka, M. Holl, H. C. Kozer, J. Lee, A. Lennarz, H. Matsubara, K. Miki, S. E. A. Orrigo, T. Suzuki, A. Tamii, and J. H. Thies, Phys. Rev. C **84**, 051305(R) (2011).
[13] J. H. Thies, D. Frekers, T. Adachi, M. Dozono, H. Ejiri, H. Fujita, Y. Fujita, M. Fujiwara, E.-W. Grewe, K. Hatanaka, P. Heinrichs, D. Ishikawa, N. T. Khai, A. Lennarz, H. Matsubara, H. Okamura, Y. Y. Oo, P. Puppe, T. Ruhe, K. Suda, A. Tamii, H. P. Yoshida, and R. G. T. Zegers, Phys. Rev. C **86**, 014304 (2012).
[14] D. Frekers, P. Puppe, J. H. Thies, and H. Ejiri, Nucl. Phys. A **916**, 219 (2013).
[15] I. Hamamoto and H. Sagawa, Phys. Rev. C **62**, 024319 (2000).
[16] D. R. Bes, O. Civitarese, and J. Suhonen, Phys. Rev. C **86**, 024314 (2012).
[17] O. Civitarese and J. Suhonen, Phys. Rev. C **89**, 044319 (2014).
[18] D. Frekers, M. Alanssari, H. Ejiri, M. Holl, A. Poves, and J. Suhonen, Phys. Rev. C **95**, 034619 (2017).
[19] J. Hyvärinen and J. Suhonen, Phys. Rev. C **91**, 024613 (2015).
[20] J. Hyvärinen and J. Suhonen, Adv. High Energy Phys. **2016**, 4714829 (2016).
[21] F. Šimkovic, V. Rodin, A. Faessler, and P. Vogel, Phys. Rev. C **87**, 045501 (2013).
[22] A. Bohr and B. R. Mottelson, *Nuclear Structure*, Vol. 1 (Benjamin, New York, 1969).
[23] K. Holinde, Phys. Rep. **68**, 121 (1981).
[24] J. Suhonen, *From Nucleons to Nucleus: Concepts of Microscopic Nuclear Theory* (Springer, Berlin, 2007).
[25] J. Suhonen, Nucl. Phys. A **563**, 205 (1993).
[26] J. Suhonen, T. Taigel, and A. Faessler, Nucl. Phys. A **486**, 91 (1988).
[27] Computer code NUDAT 2.6, Brookhaven National Laboratory, online [http://www.nndc.bnl.gov/nudat2/].
[28] M. Wang, G. Audi, A. H. Wapstra, F. G. Kondev, M. MacCormick, X. Xu, and B. Pfeiffer, Chin. Phys. C **36**, 1157 (2012).
[29] O. Civitarese, A. Faessler, and T. Tomoda, Phys. Lett. B **194**, 11 (1987).
[30] F. Šimkovic, A. Faessler, V. Rodin, P. Vogel, and J. Engel, Phys. Rev. C **77**, 045503 (2008).
[31] M. Kortelainen, O. Civitarese, J. Suhonen, and J. Toivanen, Phys. Lett. B **647**, 128 (2007).
[32] M. Kortelainen and J. Suhonen, Phys. Rev. C **75**, 051303(R) (2007).
[33] M. Kortelainen and J. Suhonen, Phys. Rev. C **76**, 024315 (2007).
[34] J. Suhonen and M. Kortelainen, Int. J. Mod. Phys. E **17**, 1 (2008).
[35] M. Aunola and J. Suhonen, Nucl. Phys. A **602**, 133 (1996).
[36] J. Suhonen, Phys. Lett. B **607**, 87 (2005).
[37] J. Suhonen and O. Civitarese, Phys. Lett. B **725**, 153 (2013).
[38] J. Suhonen and O. Civitarese, Nucl. Phys. A **924**, 1 (2014).
[39] B. Frois and I. Sick, *Modern Topics in Electron Scattering* (World Scientific, Singapore, 1991).
[40] G. F. Bertsch, D. Cha, and H. Toki, Phys. Rev. C **24**, 533 (1981).
[41] F. Krmpotic, K. Ebert, and W. Wild, Nucl. Phys. A **342**, 497 (1980).